Progress In Electromagnetics Research Letters, Vol. 89, 127–132, 2020

Evaluation of the Flux Linkage between Equally Sized Circular Loops Placed on a Layered Soil

Mauro Parise*

Abstract—This paper presents an efficient method for evaluating the flux linkage between two circular loops located on the top surface of a plane multilayer soil. The method consists of a rigorous procedure, which leads to expressing the flux as a sum of products of Bessel functions. First, the integral representation for the mutual inductance is cast into a form where the integration range is continued to the negative real axis. Subsequently, the non-oscillating part of the integrand is replaced with a rational approximation, arising from using a well-known least squares-based fitting algorithm. Finally, analytical integration is performed by applying the theorem of residues. As a result of the proposed method, the flux linkage between the loops is expressed as a finite sum of products of Bessel functions. Since no assumptions are made in the mathematical derivation, the obtained explicit expression is valid regardless of the operating frequency. Numerical tests are performed to show the advantages of the proposed method with respect to standard numerical integration techniques. In particular, it is seen how the use of the derived series representation for the inductance with 50 terms permits to achieve the same accuracy as conventional Gauss-Kronrod numerical integration technique, with the advantage of reducing the computation time by at least 8 times.

1. INTRODUCTION

It is well known that the electromagnetic (EM) and geometric properties of the subsurface structure of a terrestrial area may be inferred by interpreting measurements of the mutual impedance of a transmitter-receiver loop system through matching with theoretical response curves [1–25]. In particular, information about the earth structure may be acquired from solving the nonlinear inverse problem of searching for a layered earth model that can reproduce a recorded finite set of observations, associated with a discrete set of frequencies [4, 5, 9, 16]. Standard iterative procedures for solving nonlinear inverse problems imply a number of forward problems to be solved within an optimization loop [25]. It turns out that the efficiency of the inversion algorithm is strictly related to the availability of rigorous methods that allow to fast and accurately evaluate the mutual impedance of two loops located on a layered earth. In spite of the importance of this task, so far no explicit expressions have been derived which describe the inductive coupling between the loops, not even under the assumption of electrically and physically small loops [2, 6, 7, 14, 15, 17, 18, 21] or in the quasi-static frequency limit [6, 10, 11, 13, 23], where the effects of the displacement currents in both the air and the ground are negligible. Thus, to date, the field integral describing the inductive coupling may be evaluated only by resorting to numerical integration, but this approach has the disadvantage of being time consuming, especially in the special case where both the transmitter and receiver are placed on the layered medium [6, 23].

This paper presents a hybrid analytical-numerical procedure that allows to derive an explicit expression for the mutual inductance between two identical loops lying on the top surface of a layered conductive soil. The derived expression is not subject to restrictions on frequency and/or the size of

Received 26 November 2019, Accepted 14 January 2020, Scheduled 28 January 2020
* Corresponding author: Mauro Parise (m.parise@unicampus.it).
The author is with the University Campus Bio-Medico of Rome, Via Alvaro del Portillo 21, 00128 Rome, Italy.

the loops, and is less time consuming than conventional numerical integration algorithms like Gauss-Kronrod quadrature rule. The expression is obtained by casting the integral representation for the mutual inductance into a form where the range of integration is extended to the negative real axis. Next, the non-oscillating part of the integrand is replaced with its rational approximation according to the least squares-based fitting procedure proposed by Gustavsen [26]. This leads to expressing the original semi-infinite integral as a sum of simpler contour integrals around the pole singularities of the rational approximation. Finally, the theorem of residues is applied to each contour integral, and the mutual inductance is given as a finite sum of product of Bessel functions. Numerical tests are carried out to illustrate the advantages of the proposed approach with respect to Gauss-Kronrod quadrature rule.

2. PROBLEM FORMULATION

The problem under consideration is illustrated in Fig. 1. Two identical thin-wire circular loops, with radius a, are placed on a conducting N-layer medium and are separated by the radial distance ρ. The dielectric permittivity and electrical conductivity of the nth layer are indicated with ϵ_n and σ_n, respectively, while the magnetic permeability is assumed to be everywhere equal to that of free space μ_0. The complete integral expression describing the flux linkage per unit current between the loops is well known and given by [6]

$$M = 2\pi\mu_0 a^2 \int_0^\infty \frac{1}{u_0 + \hat{u}_1} \left[J_1(\lambda a)\right]^2 J_0(\lambda\rho)\lambda \, d\lambda, \tag{1}$$

where $J_0(\xi)$ and $J_1(\xi)$ are respectively the zeroth- and first-order Bessel functions, and t $\hat{u}_n$ are given by the recurrence relation

$$\hat{u}_n = u_n \frac{\hat{u}_{n+1} + u_n \tanh(u_n d_n)}{u_n + \hat{u}_{n+1}\tanh(u_n d_n)}, \qquad n = N-1, \ldots, 1, \tag{2}$$

with $d_1, d_2, \ldots, d_{N-1}$ being the thicknesses of the $N-1$ finite layers, and $\hat{u}_N = u_N$, with

$$u_n = \sqrt{\lambda^2 - \omega^2\mu_0\epsilon_n + j\omega\mu_0\sigma_n}. \tag{3}$$

The scope of the present section is to derive an explicit expression for the integral representation in Eq. (1). To this end, we first let

$$f(\lambda) = \frac{1}{u_0 + \hat{u}_1} \tag{4}$$

and substitute in Eq. (1) the identity [27, 28]

$$J_0(\lambda\rho) = \frac{1}{2}\left[H_0^{(1)}(\lambda\rho) - H_0^{(1)}(\bar{\lambda}\rho)\right], \tag{5}$$

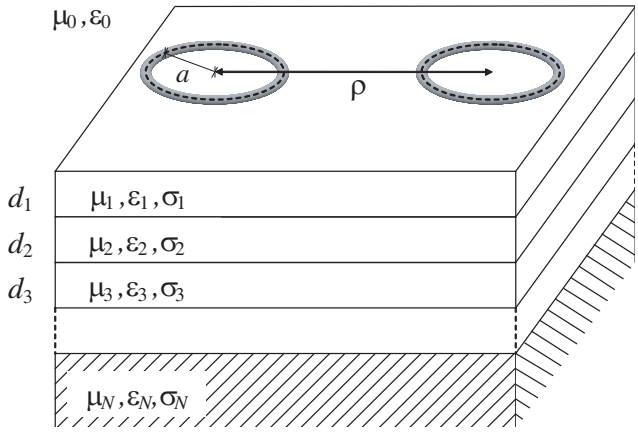

Figure 1. Two circular loops on a layered ground.

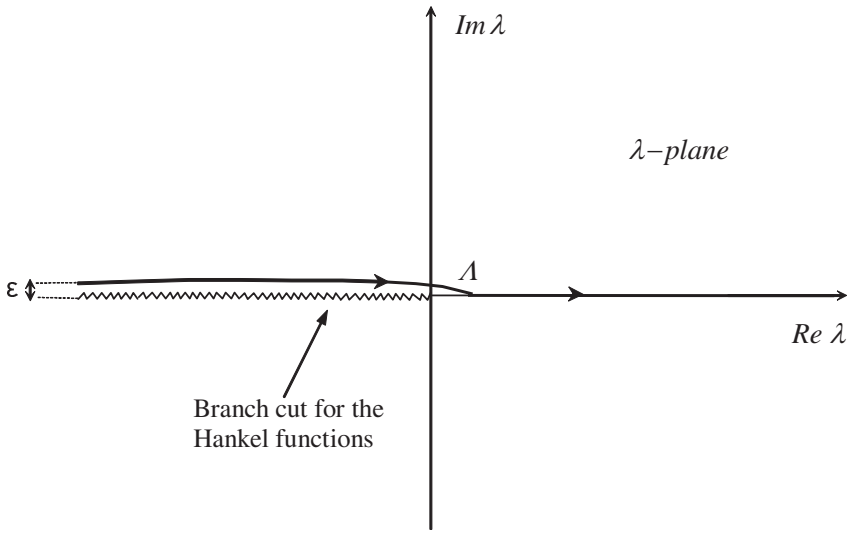

Figure 2. Integration contour in the complex λ-plane.

with $\bar{\lambda} = \lambda \exp(j\pi)$ and $H_0^{(1)}(\cdot)$ being the zeroth-order Hankel function of the first kind. It turns out that

$$\begin{aligned} M &= \pi\mu_0 a^2 \left\{ \int_0^{\infty} f(\lambda) \left[J_1(\lambda a)\right]^2 H_0^{(1)}(\lambda\rho)\lambda \, d\lambda + \int_{\infty\, e^{j\pi}}^{0} f\left(\bar{\lambda}\right) \left[J_1\left(\bar{\lambda} a\right)\right]^2 H_0^{(1)}\left(\bar{\lambda}\rho\right) \bar{\lambda} \, d\bar{\lambda} \right\} \\ &= \pi\mu_0 a^2 \int_{\Lambda} f(\lambda) \left[J_1(\lambda a)\right]^2 H_0^{(1)}(\lambda\rho)\lambda \, d\lambda, \end{aligned} \tag{6}$$

where the integration path Λ, shown in Fig. 2, is constituted by the positive real λ-axis plus the upper shore of the negative real λ-axis. Next, we introduce the rational approximation

$$f(\lambda) \cong \sum_{l=1}^{L} \frac{c_l}{j\lambda^2 - \alpha_l}, \qquad Re[\alpha_l] < 0, \tag{7}$$

arising from applying the least squares-based fitting procedure described in [26]. This allows to deform the integration contour to the upper infinite semi-circumference of the complex λ-plane, plus a number of infinitesimal circles surrounding the pole singularities exhibited by Eq. (7) in the upper half of the complex plane. Since the integrand decays exponentially when increasing $|\lambda|$ in the first and second quadrants, it turns out that the contribution to the integral in Eq. (6) due to the semi-circumference is identically null. As a consequence, Eq. (6) may be rewritten as

$$M = -\, j\pi\mu_0 a^2 \sum_{l=1}^{L} c_l \int_{\Lambda_l} \frac{1}{\lambda^2 + j\alpha_l} \left[J_1(\lambda a)\right]^2 H_0^{(1)}(\lambda\rho)\lambda \, d\lambda, \tag{8}$$

where Λ_l is the infinitesimal circle around the point $\lambda_l = \sqrt{-j\alpha_l}$, which is the lth pole of Eq. (7) belonging to the upper half of the complex λ-plane. Analytical evaluation of the lth integral on the right-hand side of Eq. (8) is straightforward by means of the theorem of residues. It reads

$$\int_{\Lambda_l} \frac{1}{\lambda^2 - \lambda_l^2} \left[J_1(\lambda a)\right]^2 H_0^{(1)}(\lambda\rho)\lambda \, d\lambda = 2\pi j \lim_{\lambda \to \lambda_l} \frac{\lambda - \lambda_l}{\lambda^2 - \lambda_l^2} \left[J_1(\lambda a)\right]^2 H_0^{(1)}(\lambda\rho)\lambda = \pi j \left[J_1(\lambda_l a)\right]^2 H_0^{(1)}(\lambda_l \rho), \tag{9}$$

and the flux linkage per unit current between the loops assumes the explicit form

$$M = \mu_0 \pi^2 a^2 \sum_{l=1}^{L} c_l \left[J_1(\lambda_l a)\right]^2 H_0^{(1)}(\lambda_l \rho). \tag{10}$$

3. DISCUSSION

To validate the proposed method, expression (10) is first applied to the calculation of the mutual inductance between two loops, 1 m in radius, situated on a two-layer medium with $\epsilon_1=\epsilon_2=10\epsilon_0$, $\sigma_1=1$ mS/m, and $\sigma_2=100$ mS/m. The radial distance ρ between the centers of the loops is taken to be equal to 15 m, and the mutual inductance is computed as a function of frequency. Four amplitude-frequency spectra are generated, each one corresponding to a different length of the sum of partial fractions in Eq. (7) generated by using the fitting algorithm described in [26]. The results of the calculations, depicted in Fig. 3, are compared with those arising from numerically integrating the expression in Eq. (1). Numerical integration is carried out by applying a Gauss-Kronrod G7-K15 scheme, originating from the combination of a 7-point Gauss rule with a 15-point Kronrod rule. From the analysis of the plotted curves it emerges that increasing the order of the rational approximation of $f(\lambda)$ improves the accuracy of the result of the computation. In fact, if L grows, the curve arising from Eq. (10) approaches the outcomes from numerical quadrature, and perfect agreement is achieved when L=20. This suggests that Eq. (10) converges to the exact solution as the order L of the rational approximation is increased. Moreover, Fig. 3 also points out that convergence of Eq. (10) is faster at higher frequencies, where it suffices to use a rational approximation made up of only 7 partial fractions to achieve highly accurate results. This aspect is confirmed by Fig. 4, which shows the relative error that originates from applying Eq. (10) rather than the G7-K15 quadrature formula, plotted versus frequency.

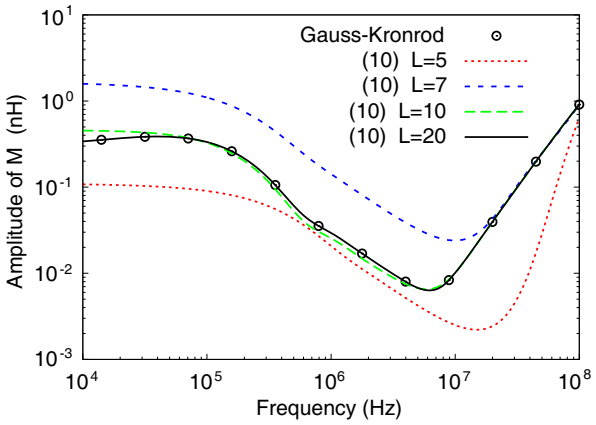

Figure 3. Amplitude-frequency spectrum of the mutual inductance between two loops.

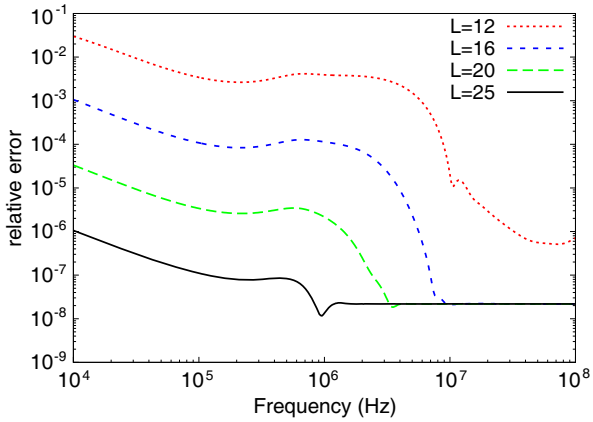

Figure 4. Relative error of the outcomes from (10) as compared to G7-K15 data, plotted against frequency.

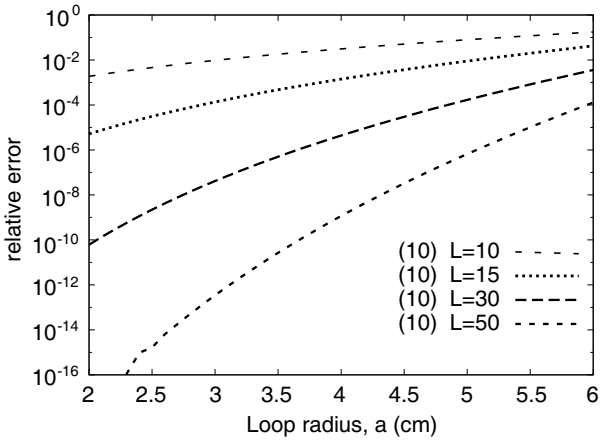

Figure 5. Relative error of the results provided by (10), as compared to G7-K15 data.

Table 1. CPU time comparisons for the computation of M.

Approach	average CPU time [s]	Speed-Up
Numerical Integration	27.4	-
(10) with $L = 10$	$2.49 \cdot 10^{-3}$	$11 \cdot 10^{3}$
(10) with $L = 15$	$6.58 \cdot 10^{-3}$	$4.16 \cdot 10^{3}$
(10) with $L = 30$	$9.26 \cdot 10^{-2}$	$2.96 \cdot 10^{2}$
(10) with $L = 50$	3.12	8.78

As seen, for most of the considered values of L the relative error dramatically drops at frequencies higher than about 1 MHz. Opposite conclusions can be drawn when changing the loop radius a in place of frequency. This point is illustrated in Fig. 5, which depicts profiles of the relative error versus a, under the assumption that the loop-to-loop spacing is ρ=15 cm and that the operating frequency is 10 MHz. The same material medium as in the previous example is considered. As can be observed, for any length L of the sum of partial fractions the error grows monotonically as a is increased. Furthermore, the curves plotted in Fig. 5 show how increasing L always makes the relative error decrease, even if the error reduction is less and less pronounced as the loop radius grows. With accuracy being equal, one would ask if Eq. (10) is advantageous in terms of computation time over numerical integration. This point is clarified by Table 1, which illustrates the average CPU time taken by the two approaches to calculate the trends of $|M|$ shown in Fig. 3. Table 1 also shows the speed-up exhibited by the proposed method, that is the ratio of the time required by the G7-K15 numerical scheme to that taken by Eq. (10). It is observed that use of Eq. (10) with L=50 terms instead of numerically integrating Eq. (1) makes it possible to reduce the time cost by at least 8 times.

4. CONCLUSIONS

This paper has presented an efficient method for calculating the mutual inductance of two circular loops lying on the surface of a plane layered conducting medium. The method leads to expressing the flux as a sum of products of Bessel functions, and consists of casting the integral representation for the mutual inductance into a form where the integration range is continued to the negative real axis. Next, the non-oscillating part of the integrand is approximated by a rational function, and analytical integration is carried out by applying the theorem of residues. Numerical simulations have been performed to illustrate the advantages of the proposed technique over standard numerical integration schemes.

REFERENCES

1. Boerner, D. E., "Controlled source electromagnetic deep sounding: Theory, results and correlation with natural source results," *Surveys in Geophysics*, Vol. 13, No. 4–5, 435–488, 1992.
2. Parise, M., "Exact electromagnetic field excited by a vertical magnetic dipole on the surface of a lossy half-space," *Progress In Electromagnetics Research B*, Vol. 23, 69–82, 2010.
3. Kong, F. N., S. E. Johnstad, and J. Park, "Wavenumber of the guided wave supported by a thin resistive layer in marine controlled-source electromagnetics," *Geophysical Prospecting*, Vol. 29, No. 10, 1301–1307, 2003.
4. Shastri, N. L. and H. P. Patra, "Multifrequency sounding results of laboratory simulated homogeneous and two-Layer earth models," *IEEE Trans. Geosci. Remote Sensing*, Vol. 26, No. 6, 749–752, 1988.
5. Farquharson, C. G., D. W. Oldenburg, and P. S. Routh, "Simultaneous 1D inversion of loop-loop electromagnetic data for magnetic susceptibility and electrical conductivity," *Geophysics*, Vol. 68, No. 6, 1857–1869, 2003.
6. Ward, S. H. and G. W. Hohmann, "Electromagnetic theory for geophysical applications," *Electromagnetic Methods in Applied Geophysics, Theory — Volume 1*, 131–308, edited by M. N. Nabighian, SEG, Tulsa, Oklahoma, 1988.

7. Zhdanov, M. S., *Geophysical Electromagnetic Theory and Methods*, Elsevier, Amsterdam, 2009.
8. Parise, M., V. Tamburrelli, and G. Antonini, "Mutual impedance of thin-wire circular loops in near-surface applications," *IEEE Trans. on Electromagnetic Compatibility*, Vol. 61, No. 2, 558–563, 2019.
9. Beard, L. P. and J. E. Nyquist, "Simultaneous inversion of airborne electromagnetic data for resistivity and magnetic permeability," *Geophysics*, Vol. 63, No. 5, 1556–1564, 1998.
10. Parise, M., "Quasi-static vertical magnetic field of a large horizontal circular loop located at the earth's surface," *Progress In Electromagnetics Research Letters*, Vol. 62, 29–34, 2016.
11. Wait, J. R., "Mutual electromagnetic coupling of loops over a homogeneous ground," *Geophysics*, Vol. 20, No. 3, 630–637, 1955.
12. Tiwari, K. C., D. Singh, and M. K. Arora, "Development of a model for detection and estimation of depth of shallow buried non-metallic landmine at microwave x-band frequency," *Progress In Electromagnetics Research*, Vol. 79, 225–250, 2008.
13. Telford, W. M., L. P. Geldart, and R. E. Sheriff, *Applied Geophysics*, Cambridge University Press, Cambridge, UK, 1990.
14. Parise, M., "An exact series representation for the EM field from a circular loop antenna on a lossy half-space," *IEEE Antennas and Wireless Propagation Letters*, Vol. 13, 23–26, 2014.
15. Parise, M., "Full-wave analytical explicit expressions for the surface fields of an electrically large horizontal circular loop antenna placed on a layered ground," *IET Microwaves, Antennas & Propagation*, Vol. 11, 929–934, 2017.
16. Palacky, G. J., "Resistivity characteristics of geologic targets," *Electromagnetic Methods in Applied Geophysics*, Vol. 1, 52–129, Nabighian, M. N., Ed., SEG, Tulsa, Oklahoma, 1988.
17. Parise, M., "On the surface fields of a small circular loop antenna placed on plane stratified earth," *International Journal of Antennas and Propagation*, Vol. 2015, 1–8, 2015.
18. Singh, N. P. and T. Mogi, "Electromagnetic response of a large circular loop source on a layered earth: A new computation method," *Pure and Applied Geophysics*, Vol. 162, 181–200, 2005.
19. Parise, M., "Efficient computation of the surface fields of a horizontal magnetic dipole located at the air-ground interface," *International Journal of Numerical Modelling: Electronic Networks, Devices and Fields*, Vol. 29, 653–664, 2016.
20. Parise, M. and G. Antonini, "On the inductive coupling between two parallel thin-wire circular loop antennas," *IEEE Trans. on Electromagnetic Compatibility*, Vol. 60, No. 6, 1865–1872, 2018.
21. Singh, N. P. and T. Mogi, "Effective skin depth of EM fields due to large circular loop and electric dipole sources," *Earth Planets Space*, Vol. 55, 301–313, 2003.
22. Parise, M., "On the use of cloverleaf coils to induce therapeutic heating in tissues," *Journal of Electromagnetic Waves and Applications*, Vol. 25, Nos. 11–12, 1667–1677, 2011.
23. Ryu, J., H. F. Morrison, and S. H. Ward, "Electromagnetic fields about a loop source of current," *Geophysics*, Vol. 35, No. 5, 862–896, 1970.
24. Parise, M., "Fast computation of the forward solution in controlled-source electromagnetic sounding problems," *Progress In Electromagnetics Research*, Vol. 111, 119–139, 2011.
25. Constable, S. C., R. L. Parker, and C. G. Constable, "Occam's inversion: A practical algorithm for generating smooth models from electromagnetic sounding data," *Geophysics*, Vol. 52, No. 3, 289–300, 1987.
26. Gustavsen, B. and A. Semlyen, "Rational approximation of frequency domain responses by vector fitting," *IEEE Transactions on Power Delivery*, Vol. 14, 1052–1061, 1999.
27. Parise, M., "A highly accurate analytical solution for the surface fields of a short vertical wire antenna lying on a multilayer ground," *Waves in Random and Complex Media*, Vol. 28, 49–59, 2018.
28. Parise, M., "Improved Babylonian square root algorithm-based analytical expressions for the surface-to-surface solution to the Sommerfeld half-space problem," *IEEE Transactions on Antennas and Propagation*, Vol. 63, 5832–5837, 2015.